

Enhanced crack-bridging by unbonded inclusions in a brittle matrix

H.W. Chandler^{a,*}, I.J. Merchant^a, R.J. Henderson^a, D.E. Macphee^b

^a*Department of Engineering, Fraser Noble Building, University of Aberdeen, Aberdeen AB24 3UE, UK*

^b*Department of Chemistry, Meston Building, University of Aberdeen, Aberdeen AB24 3UE, UK*

Received 23 August 2000; received in revised form 23 February 2001; accepted 4 March 2001

Abstract

A method of engineering the microstructure of brittle composites is proposed and tested that improves the effectiveness of non-fibrous inclusions to bridge cracks in the matrix. This microstructure consists of a continuous matrix of brittle material surrounding brittle inclusions that are not bonded to it. In order to demonstrate that this works, a series of experiments have been performed with model cement systems, including aggregates such as: coated and uncoated sand; spherical and angular glass; and expanded polystyrene balls. The results have shown that the interfacial bonding between the inclusions and the matrix controls the crack path through the composite and determines whether or not an inclusion will act as a bridge and consequently provide a toughening effect. Specifically, when a moderately strong bond is present the crack path is such as to reduce the number of bridging inclusions. However, when there is no bond at all, the matrix crack follows a flatter path and more inclusions bridge the crack. Nevertheless bridging is only effective with non-spherical particles. The experimental results also suggest, that whilst the initial toughness is reduced by very weak interfaces, such composites are most likely to exhibit rising toughness behaviour. The technological implications for cementitious and refractory materials are discussed. © 2001 Elsevier Science Ltd. All rights reserved.

Keywords: Cement; Mechanical properties; Microstructure; Structural applications

1. Introduction

1.1. Background

The resistance to crack propagation in brittle materials is a key material property for many engineering applications, particularly those involving severe thermal shock.^{1–3} In many such applications the expected tensile stress may be in excess of the tensile strength so any residual strength is important.⁴ This residual strength is influenced by the toughness, and the way it varies as the crack extends. In particular, it seems advantageous to have easy propagation while a crack is small and progressively greater resistance to propagation as it lengthens.⁴ Rather than one large crack, this will result in a large number of small cracks that act to reduce the elastic stiffness and consequently the thermal stress, without inducing complete loss of strength.⁵

Increasing toughness with crack growth has been observed in a number of types of traditional ceramics. Incorporation of non-fibrous particles into a glassy

matrix was possibly used originally as a way to reduce shrinkage or reuse scrap. However, it has been found to be beneficial, specifically: in the refractories industry;⁶ in brick making;^{7,8} in clay crucibles;⁹ in porcelain articles¹⁰ and in coarse pottery at least since Roman times.¹¹ A recent example in refractories is the use of large magnesia grains (MgO) in a fine matrix consisting of MgO and spinel (MgO–Al₂O₃).^{12,13} The precise mechanism is not clear but it is known that residual stresses in the microstructure lead, in some way, to increased toughness perhaps through grain bridging.

1.2. Improving the effectiveness of short inclusions

Like fibres, particulate inclusions can be effective in hindering the opening of the crack faces by sometimes providing kinematic constraints (see Fig. 1a). Even with a suitable choice of particulate, however, an increase in toughness is not guaranteed, as is observed when coarse magnesia grains are added to a fine magnesia matrix¹⁴ (see Fig. 1b). In order to provide this kinematic constraint the inclusions must clearly be non-spherical (see Fig. 1c). The key to engineering rising crack growth using non-fibrous inclusions would be to maximise the number of inclusions intercepted by large propagating

* Corresponding author. Tel.: +44-1224-272-496; fax: +44-1224-272-496.

E-mail address: h.w.chandler@eng.abdn.ac.uk (H.W. Chandler).

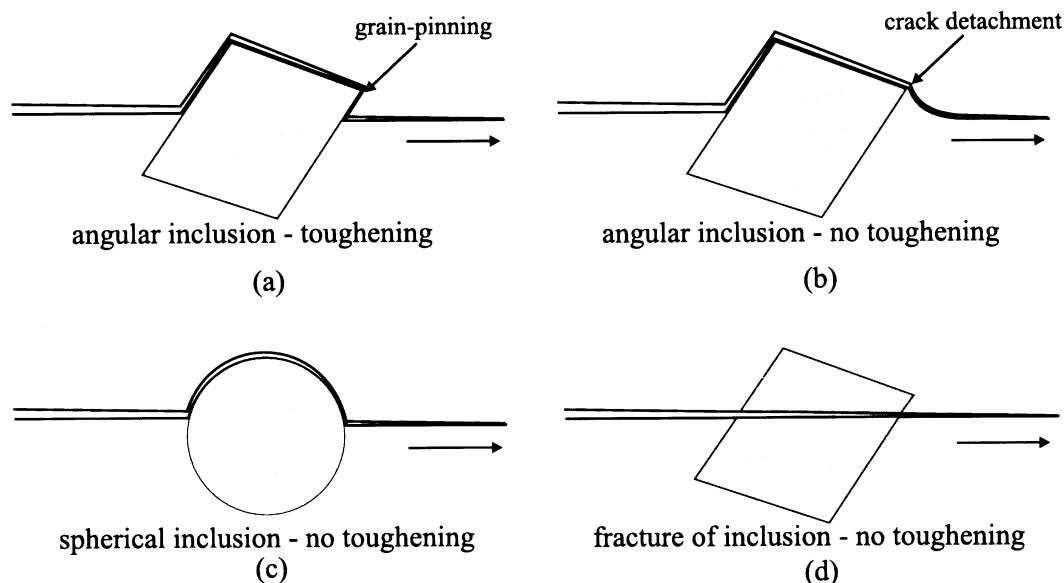


Fig. 1. Fracture paths around particulate inclusions. The arrow indicates the direction of crack propagation: (a) shows a flat crack path following the shape of the inclusion; (b) shows the detachment of the crack where an inclusion is strongly bonded to the matrix; (c) shows that no pinning can take place with spherical inclusions, as does (d), when an inclusion is fractured.

cracks, in such a way that this pinning role is optimised. To do this we need to understand crack paths.

Much work has been published concerning the path of cracks propagating along, away from or approaching an interface between two materials.^{15–17} This work is largely restricted to the two-dimensional case and is not sufficiently advanced to be any more than a guide to the three-dimensional interactions of cracks with discrete inclusions. It is clear, however, that the elastic and fracture properties of the two materials and the interface are important as well as the presence of residual stress. At the simplest level the following is likely to be true when residual stresses are not present:

- A strong interfacial bond with any brittle inclusion may lead to the crack continuing through the inclusion producing virtually no toughening enhancement (Fig. 1d).
- A weaker bond with the inclusion might lead to a more complex and, at our current level of understanding, less predictable crack path. For example, if the bond is weak enough for the crack to propagate along the interface, the point at which the crack detaches from the interface is important as it will control how much pinning occurs (Fig. 1b).
- The behaviour with unbonded particles may be radically different. Cracks in solids with a high level of isolated porosity tend to follow relatively undeviated paths. (Readers can demonstrate this by breaking a bar of foamed confectionery.) If unbonded particles were present, then cracks propagating through the matrix would interact with them as if they were holes, giving rise to a similar

fracture path. We shall refer to this as flat fracture in this paper. As the crack faces open, however, at least a proportion of the particles would bridge the two crack faces and start to hinder further crack opening (Fig. 1a).

Consideration of these points led us to the following hypothesis:

The incorporation of non-spherical particles into a brittle matrix, that are unbonded to the matrix, gives rise to a flat fracture-path that promotes crack-pinning and leads to a rising toughness curve.

2. Experimental

The aim of the experiments reported below was to show, in line with the above hypothesis, that:

1. A flat fracture surface is produced in hardened cement even when a large volume fraction of isolated holes are present.
2. The fracture surface is still flat when unbonded particles are present but is perturbed when the particles are bonded.
3. Using spherical particles gives rise to no increase in toughness with crack growth.
4. Using non-spherical particles gives an increase in toughness with crack growth as long as the crack follows a locally flat path (i.e. as it passes an individual inclusion).

To do this we fabricated a range of cement mortars changing the aggregate and the interfacial strength.

2.1. Materials

Ordinary Portland cement (OPC)^a was used as the matrix throughout this work. This was made always with distilled water with a water-to-cement ratio of 0.3 (by weight).

To demonstrate the occurrence of flat fracture paths in a brittle matrix two specimens were fabricated. Firstly, a batch of ordinary Portland cement was formed by itself. Secondly, a batch using ordinary Portland cement and expanded polystyrene spheres^b was made to incorporate a high level of large-scale porosity. The stiffness of the polystyrene is so low in comparison with the cement that it behaves as if it were not present.

In order to demonstrate the difference between mortars with bonded and unbonded aggregates DA 8/16 Leighton Buzzard sand^c (1–2 mm) was used to fabricate them. Two batches were made, one with sand in the as received condition and one with sand coated with a thin layer of candle wax in order to prevent any significant bonding taking place during hydration. The wax coating was achieved by adding a small quantity of melted candle wax to the sand which had been pre-heated to 70°C. This ensured that the wax did not solidify immediately, allowing complete wetting of the sand grains. The mixture was then cooled slowly while being tumbled to discourage the grains sticking together. The thickness of the wax layer was in the region of 20 µm, measured using optical microscopy.

Two further batches were used to demonstrate the effect of using spherical particles compared with angular particles. Soda-lime-silica glass was used because:

- the interfacial bond between it and cement is known to be very weak¹⁸ and was in this case sufficiently weak to give flat fracture;
- it was obtainable both as near spherical ballotini^d and as debris from broken toughened glass plates^e

To make the test specimens the aggregate (coated or uncoated) and cement were mixed together with water in a domestic food mixer. The batch details are shown in Table 1. The batches were cast into steel moulds to form notched plates (150×75×30 mm) or bars (25×25×150 mm) and vibrated on a casting table in order to remove almost all the air bubbles. The plates and bars, on de-moulding, were cured in a high humidity environment prior to testing at 28 days.

^a Donated by Blue Circle Industries plc, Dunbar Works, East Lothian, Scotland.

^b Obtained from The John Lewis Partnership, Aberdeen, Scotland.

^c Obtained from Hepworth Minerals and Chemicals, Heath and Reach, England.

^d Obtained from Potters-Ballotini Ltd, Barnsley, England.

^e Donated by Adshel, Aberdeen, Scotland.

2.2. Testing

Fracture toughness tests were carried out on the notched plates using a test developed for brittle materials.^{19,20} The test has a double cantilever geometry and the crack is propagated by applying two compressive loads on the end of the specimen parallel to the crack, such as to provide a bending moment in the cantilevers. The crack was extended by the application of a load using an Instron 1185 universal testing machine. The test was carried out with a cross-head displacement of 0.2 mm/min. The crack extension was measured visually. The test arrangement can be seen in Fig. 2 and calculation of

Table 1
Details of the various batches

Batch ^a	Aggregate type	OPC		Aggregate		\bar{D} (mm)	w/c
		(vol.%)	(wt.%)	(vol.%)	(wt.%)		
BS	DA8/16 sand	29.9	50.0	36.1	50.0	1–2	0.3
US	Wax coated DA 8/16 sand	29.5	50.0	35.4	50.0	1–2	0.3
SG	Spherical glass	29.5	50.0	39.3	50.0	3	0.3
AG	Angular glass	29.5	50.0	39.3	50.0	3–4	0.3
EP	Expanded polystyrene	28.8	96.0	37.0	4.0	5	0.3
OPC	–	47.4	100.0	0.0	0.0	–	0.3

^a BS indicates the sand is bonded to the matrix and US that the wax coating has prevented bonding. SG and AG are mortars made with unbonded spherical and angular glass respectively. EP is a mortar made with expanded polystyrene, while OPC is a standard ordinary Portland cement batch. \bar{D} is the average grain diameter of the aggregate and w/c is the water-to-cement ratio by weight. Note: the remainder of the volume added to the batches consisted of water.

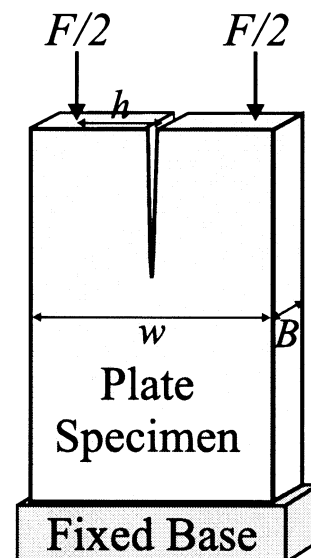


Fig. 2. The arrangement for the fracture toughness tests. F is the applied load, h is half of the distance between the loading points, w is the width of the plate, ν is the Poisson's ratio and B is the thickness of the plate.

the apparent toughness made using the expression below.

$$K_{\text{app}} = \frac{F}{\sqrt{w}} \left(\frac{h}{w} - \frac{1}{4} \right) \sqrt{2} \sqrt{\frac{12}{1 - \nu^2}} \frac{1}{B} \quad (1)$$

where F is the applied load, h is half of the distance between the loading points, w is the width of the plate, ν is the Poisson's ratio and B is the thickness of the plate.

On completion of the fracture toughness test, the two portions of the notched plate were separated. Analysis of the fracture surfaces was carried out to demonstrate the differences in the area percentage of mortar visible on the crack surface. This was done by point counting while observing the surface of the fractured plates under a low powered microscope. Specifically, a system of cross hairs was placed just above the surface of the mortar. The point under the cross hairs was then categorised as a sand grain, a hole where a sand grain had been, cement matrix or an air bubble in the matrix. The sample was then moved in a random pattern so that a new point was observed under the cross hairs. This was repeated until 200 random points had been observed. The results of the point counting were used to estimate the volume of hydrated cement paste, aggregate inclusions and macropores due to casting.

Stress–strain curves were produced in four-point bending by fixing a strain gauge to the tensile face. The load was applied using a Hounsfield H10KS testing machine, and the nominal stress calculated from the bending moment assuming linear elasticity. The strain was measured with a Peekal strain indicator.

3. Results and discussion

The fracture tests for plain OPC and a mortar made from uncoated sand are shown in Fig. 3. These show no significant increase in toughness as the crack grows.

As expected, the fracture tests on the specimen with expanded polystyrene aggregate gave a completely flat fracture (see Fig. 4). Once divided by the volume fraction of cement, the data gives a toughness curve equivalent to that of OPC (also divided by the volume fraction of cement).

The mortar made from the wax-coated sand was tested in a bend test and the stress–strain results are shown in Fig. 5 along with those from a mortar made from uncoated sand. The stiffness of the batch made from wax-coated sand is about half that of the bonded sand. This reduction may be attributed to the holes containing the sand grains acting as empty pores. This clearly demonstrates that, as we had hoped, the sand grains are indeed unbonded.

The results of the toughness test on the mortar made with wax-coated sand are shown in Fig. 4. The initial

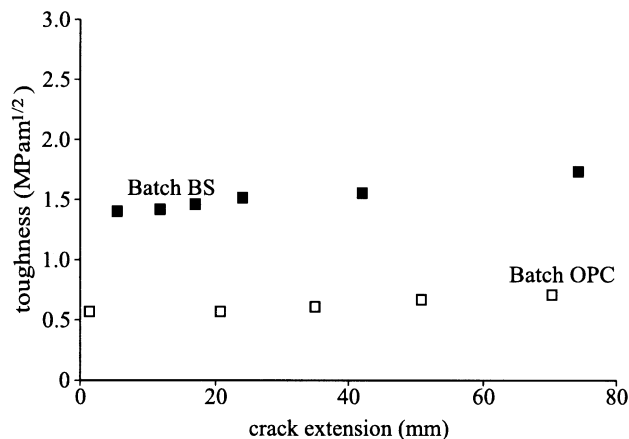


Fig. 3. Toughness curves for the ordinary Portland cement batch (□ OPC) and the mortar with bonded DA8/16 sand (■ BS).

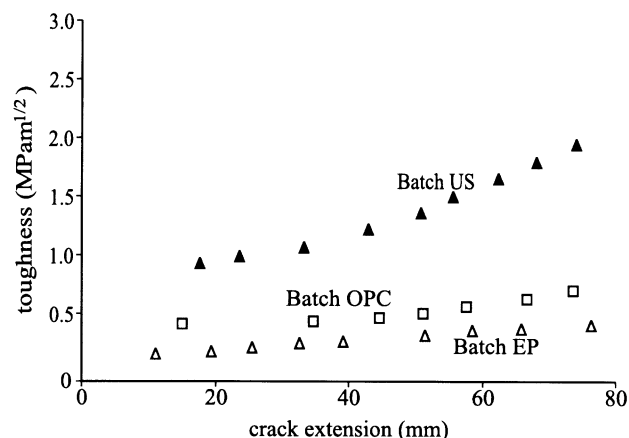


Fig. 4. Toughness curves for ordinary Portland cement (□ OPC), a batch made with an aggregate of expanded polystyrene (△ EP), and a mortar batch made with wax coated DA8/16 sand (▲ US).

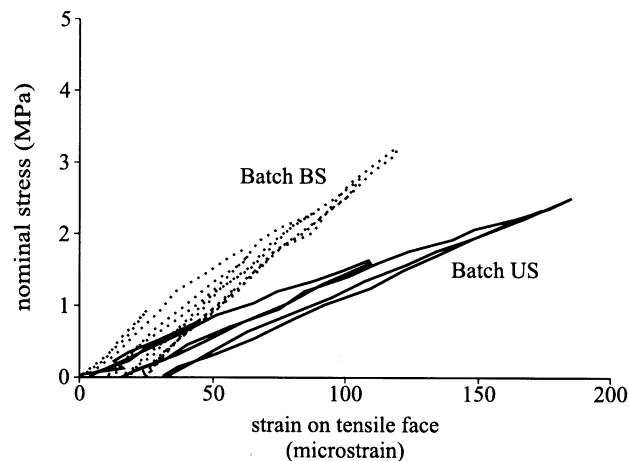


Fig. 5. Stress–strain curves for the bonded sand mortar (BS) and the wax coated sand mortar (US). The strain is measured on the tensile face during a four-point bend test.

toughness is in fact lower than the bonded sand, as observed in other cementitious materials,²¹ but it can be seen that as the crack grows the toughness increases. Clearly as the crack faces open the action of the grains pinning the faces together causes this increase.

The results from the tests on mortars made from glass aggregates are shown in Fig. 6. As predicted the inclusion of spherical aggregate, even though unbonded or weakly bonded to the matrix, produces a flat toughness curve. The spherical aggregate is unable to pin the faces together, and, therefore, cannot increase the toughness as the crack grows. When angular glass aggregate is used in the batches there is still very little bonding between the aggregate and the cement matrix. However, now the angular shape of the grains is able to pin the crack faces together and produce rising toughness as the crack grows.

The results of visual analysis of the surfaces, shown in Table 2, demonstrate the effect the coating had on the crack path. Table 2 shows the percentages of sand grains, S , holes created by the pull-out of the sand grains, H and the sum of these components, $S+H$. In contrast to this the matrix components are shown in the form of cement matrix, M , air-bubbles, P and once

again the sum of these, $M+P$. The summations allow a comparison to be made between the percentage of pinning inclusions ($S+H$) and the matrix ($M+P$). Compared with the control batch, BS, the batch with wax coated sand, US, had a higher percentage of visible sand grains (or holes where sand grains had pulled out) relative to the cement matrix (or pores). These results show that when the matrix is bonded to the particulate phase the crack has a tendency to avoid the interface as illustrated schematically in Fig. 1, and so reduce the likelihood of pinning.

The four key assertions are all confirmed, and thus, there is strong evidence for the hypothesis being correct. That is the wax coated sand provided a better opportunity for grain bridging. This low initial toughness and steady rise with crack growth is just what is required for minimising damage during severe thermal shock in refractory ceramics.

The role of residual stresses in fired ceramics or cementitious materials can now be discussed with this in mind:

- If particles try to shrink away from the matrix on cooling or curing then the conditions are right to produce the microstructural effects just discussed, i.e. where de-bonding takes place ahead of the crack the overall effect is similar to always having unbonded grains. This mechanism may be responsible for the rising toughness observed in the MgO-spinel composite or cements with sulphate additions discussed in earlier papers.^{14,22}
- If the matrix shrinks more than the particles on cooling then the matrix is put into a state of hoop tension near the interfaces. This tension might encourage the path of the main propagating crack towards the inclusion so increasing the total number of inclusions intercepted by the crack. If this happened the crack faces would also be pushed apart near the tip. But away from the immediate vicinity of the crack tip, the opening faces could be pinned by at least a fraction of the inclusions.²³
- Additionally, in either case there is a net expansion of the composite on relief of residual stress by microcracking. This occurs because the brittle material is much weaker in tension than in compression so the microcracking relieves residual tension. This in turn reduces residual compensating compressive stresses in the intact material resulting in a net expansion of the composite. This may also contribute to the toughening.^{14,22}

4. Conclusions

We have shown that:

- The presence of isolated holes in hardened cement gives as flat a fracture surface as dense cement.

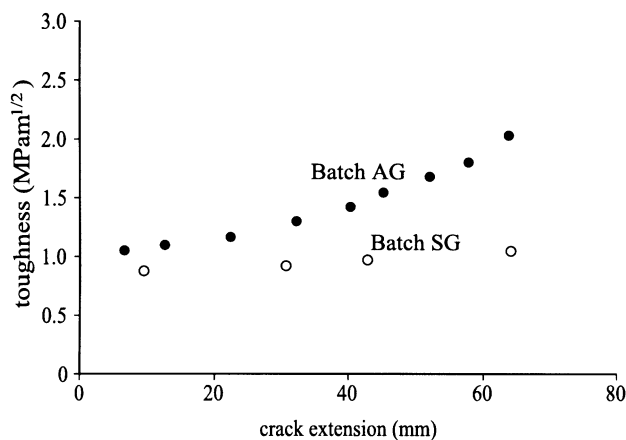


Fig. 6. Toughness curves for aggregates of spherical glass (○ SG) and angular glass (● AG). This demonstrates the difference the shape of aggregate has on the toughness curves.

Table 2
Spot counting of components present in the fracture surface

Batch	Grains, S (%)	Holes, H (%)	$S+H^a$ (%)	Cement matrix M (%)	Air bubble pores P (%)	$M+P^b$ (%)
BS	25.4	20.7	46.1	51.4	2.4	53.8
US	35.2	30.2	65.4	33.2	1.5	34.7
SG	28.6	28.6	57.2	41.0	1.9	42.9
AG	32.3	33.3	65.5	32.3	2.2	34.5
EP	33.3	25.0	58.3	38.9	2.8	41.7
OPC	0.0	0.0	0.0	96.2	3.8	100.0

^a $S+H$ is the sum of the percentage of aggregate grains, S and the pull-out holes, H .

^b $M+P$ is the sum of the percentage of visible cement matrix, M and the air bubbles, P .

- Making the particles unbonded gives a flatter fracture path compared with bonded particles.
- Using spherical particles gives rise to no increase in toughness with crack growth even if there is a flat fracture through the cement.
- Using non-spherical particles gives an increase in toughness with crack growth as long as the crack follows a flat path.

We therefore have given strong evidence that:

The incorporation of non-spherical particles into a brittle matrix, that are unbonded to the matrix, gives rise to a flat fracture-path that promotes crack-pinning and leads to a rising toughness curve.

This simple result has wide implications for the microstructural design of refractories, technical ceramics and cementitious materials. For instance it should be possible to fabricate nominally impermeable yet tough refractories by producing a dense matrix containing unbonded particulate inclusions.

Acknowledgements

The authors would like to thank EPSRC for the funding for this project. Also, they would like to thank Adshel for the supply of waste glass.

References

1. Hasselman, D. P. H., Micromechanical thermal stresses and thermal stress resistance of porous brittle ceramics. *J. Am. Ceram. Soc.*, 1969, **52**(4), 215–216.
2. Chandler, H. W., Thermal-stress in ceramics. *Br. Ceram. Trans. J.*, 1981, **80**(6), 191–195.
3. Swain, M. V., R-curve behaviour and thermal shock resistance of ceramics. *J. Am. Ceram. Soc.*, 1990, **73**(3), 621–628.
4. Larson, D. R., Coppola, J. A. and Hasselman, D. P. H., Fracture toughness and spalling of high- Al_2O_3 refractories. *J. Am. Ceram. Soc.*, 1974, **57**(10), 417–421.
5. Hasselman, D. P. H., Griffith criterion and thermal shock resistance of single-phase versus multiphase brittle ceramics. *J. Am. Ceram. Soc.*, 1969, **52**(5), 288–289.
6. Chesters, J. H., *Refractories production and properties*. The Iron and Steel Institute, London, 1973.
7. Hodges, H., *Artifacts*. Gerald Duckworth & Co., 1989, pp. 19–25.
8. Brosnan, D. A., Implications of toughening of clay on brick performance. *J. Can. Ceram. Soc.*, 1993, **62**(2), 134–138.
9. Merchant, I. J., *English Medieval Glass-making Technology: Scientific Analysis of the Evidence*. PhD thesis, University of Sheffield, 1998, pp. 114–118.
10. Sugiyama, N., Harada, H. and Ishada, H., Effect of alumina addition on the feldspathic porcelain bodies: Strengthening of feldspathic porcelain bodies by alumina. *Nippon seramikkyu kyokai gakujiutsu ronbunshi*, 1997, **105**(2), 126–130.
11. Williams, J., Li, W., Jenkins, D. A. and Livens, R. G., An analytical study of the composition of Roman coarse wares from the fort of Bryn y Gefeiliu (Caer Llugwy) in Snowdonia. *J. Arch. Sci.*, 1974, **1**, 47–67.
12. Harmuth, H. and Tschegg, E. K., A fracture mechanics approach for the development of refractory materials with reduced brittleness. *Fat. and Frac. Eng. Mater.*, 1997, **20**(11), 1585–1603.
13. Henderson, R. J., Chandler, H. W. and Strawbridge, I., A model for non-linear behaviour of refractories. *Br. Ceram. Trans. J.*, 1997, **96**(3), 85–91.
14. Henderson, R. J. and Chandler, H. W., The fracture behaviour of dual phase composite refractories. In *Engineering with Ceramics*, ed. W. E. Lee and B. Derby. British Ceramic Proceedings 59, The Institute of Materials, 1999, pp. 225–231.
15. Wang, C., Libardi, W. and Baldo, J. B., Analysis of crack extension paths and toughening in a two phase brittle particulate composite by the boundary element method. *Int. J. Fract.*, 1998, **94**(2), 177–188.
16. Hutchinson, J. W. and Suo, Z., Mixed-mode cracking in layered materials. *Advances in Applied Mechanics*, 1992, **29**, 63–91.
17. Lipetsky, P. and Knesl, Z., Crack-particle interaction in a two-phase composite. *Int. J. Fract.*, 1995, **73**(1), 81–92.
18. Bentur, A. and Diamond, S., Fracture of glass fiber reinforced cement. *Cem. Concr. Res.*, 1984, **14**(1), 31–42.
19. Browne, D. J. and Chandler, H. W., Computer design of a controlled fracture test. *Br. Ceram. Trans. J.*, 1987, **86**(6), 202–205.
20. Chandler, H. W., Henderson, R. J., Al-Zubaidy, M. N. and Muhaidi, A., A fracture test for brittle materials. *J. Eur. Ceram. Soc.*, 1997, **17**(6), 759–763.
21. Prokopski, G. and Halbiniak, J., Interfacial transition zone in cementitious materials. *Cem. Concr. Res.*, 2000, **30**(4), 579–583.
22. Chandler, H. W., Macphee, D. E., Atkinson, I., Henderson, R. J. and Merchant, I. J., Enhancing the mechanical behaviour of cement based materials. *J. Eur. Ceram. Soc.*, 2000, **20**(8), 1129–1133.
23. Ohji, T., Jeong, Y.-K., Choa, Y.-H. and Niihara, K., Strengthening and toughening mechanisms of ceramic nanocomposites. *J. Am. Ceram. Soc.*, 1998, **81**(6), 1453–1460.